LAMB WAVE PROPAGATION IN A RESTRICTED GEOMETRY COMPOSITE PI-JOINT SPECIMEN (PREPRINT)

James L. Blackshire

Nondestructive Evaluation Branch
Metals, Ceramics & NDE Division

Som Soni

Air Force Institute of Technology

NOVEMBER 2011

STINFO COPY

AIR FORCE RESEARCH LABORATORY
MATERIALS AND MANUFACTURING DIRECTORATE
WRIGHT-PATTERSON AIR FORCE BASE, OH 45433-7750
AIR FORCE MATERIEL COMMAND
UNITED STATES AIR FORCE

REPORT DOCUMENTATION PAGE		*Form Approved* *OMB No. 0704-0188*

The public reporting burden for this collection of information is estimated to average 1 hour per response, including the time for reviewing instructions, searching existing data sources, gathering and maintaining the data needed, and completing and reviewing the collection of information. Send comments regarding this burden estimate or any other aspect of this collection of information, including suggestions for reducing this burden, to Department of Defense, Washington Headquarters Services, Directorate for Information Operations and Reports (0704-0188), 1215 Jefferson Davis Highway, Suite 1204, Arlington, VA 22202-4302. Respondents should be aware that notwithstanding any other provision of law, no person shall be subject to any penalty for failing to comply with a collection of information if it does not display a currently valid OMB control number. **PLEASE DO NOT RETURN YOUR FORM TO THE ABOVE ADDRESS**.

1. REPORT DATE *(DD-MM-YY)*	2. REPORT TYPE	3. DATES COVERED *(From - To)*
November 2011	Journal Article Preprint	01 September 2011 – 01 September 2011

4. TITLE AND SUBTITLE	5a. CONTRACT NUMBER
LAMB WAVE PROPAGATION IN A RESTRICTED GEOMETRY COMPOSITE PI-JOINT SPECIMEN (PREPRINT)	In-house
	5b. GRANT NUMBER
	5c. PROGRAM ELEMENT NUMBER 62102F

6. AUTHOR(S)	5d. PROJECT NUMBER
James L. Blackshire (AFRL/RXLP) Som Soni (Air Force Institute of Technology)	4349
	5e. TASK NUMBER 40
	5f. WORK UNIT NUMBER LP110100

7. PERFORMING ORGANIZATION NAME(S) AND ADDRESS(ES)	8. PERFORMING ORGANIZATION REPORT NUMBER
Nondestructive Evaluation Branch (AFRL/RXLP) Metals, Ceramics & NDE Division Air Force Research Laboratory Materials and Manufacturing Directorate Wright-Patterson Air Force Base, OH 45433-7750 Air Force Materiel Command United States Air Force / Air Force Institute of Technology Dept. Sys. & Engineering Management (AFIT/ENV) Wright-Patterson Air Force Base, OH 45433	AFRL-RX-WP-TP-2011-4406

9. SPONSORING/MONITORING AGENCY NAME(S) AND ADDRESS(ES)	10. SPONSORING/MONITORING AGENCY ACRONYM(S)
Air Force Research Laboratory Materials and Manufacturing Directorate Wright-Patterson Air Force Base, OH 45433-7750 Air Force Materiel Command United States Air Force	AFRL/RXLP
	11. SPONSORING/MONITORING AGENCY REPORT NUMBER(S) AFRL-RX-WP-TP-2011-4406

12. DISTRIBUTION/AVAILABILITY STATEMENT
Approved for public release; distribution unlimited.

13. SUPPLEMENTARY NOTES
PAO Case Number: 88ABW 2011-4778; Clearance Date: 07 Sep 2011. Document contains color.

Journal article submitted to *Review of Progress in Quantitative NDE* 2011.

14. ABSTRACT
The propagation of elastic waves in a material can involve a number of complex physical phenomena, resulting in both subtle and dramatic effects on detected signal content. In recent years, the use of advanced methods for characterizing and imaging elastic wave propagation and scattering processes has increased, where for example the use of scanning laser vibrometry and advanced computational models have been used very effectively to identify propagating modes, scattering phenomena, and damage feature interactions. In the present effort, the propagation of Lamb waves within a narrow, constrained geometry composite pi-joint structure are studied using 3D finite element models and scanning laser vibrometry measurements, where the effects of varying sample thickness, complex joint curvatures, and restricted structure geometries are highlighted, and a and a direct comparison of computational and experimental results are provided for simulated and realistic geometry composite pi-joint samples.

15. SUBJECT TERMS
composite joint, Lamb waves, scanning laser vibrometry, finite element modeling

16. SECURITY CLASSIFICATION OF:			17. LIMITATION OF ABSTRACT:	18. NUMBER OF PAGES	19a. NAME OF RESPONSIBLE PERSON (Monitor)
a. REPORT Unclassified	b. ABSTRACT Unclassified	c. THIS PAGE Unclassified	SAR	14	Mark Blodgett 19b. TELEPHONE NUMBER (Include Area Code) N/A

Standard Form 298 (Rev. 8-98)
Prescribed by ANSI Std. Z39-18

LAMB WAVE PROPAGATION IN A RESTRICTED GEOMETRY COMPOSITE PI-JOINT SPECIMEN

James L. Blackshire[1] and Som Soni[2]

[1]Air Force Research Laboratory, Materials and Manufacturing Directorate (AFRL/RXLP), Wright-Patterson AFB, OH 45433, USA
[2]Air Force Institute of Technology, Dept. Sys. & Engineering Management (AFIT/ENV), Wright-Patterson AFB, OH 45433, USA

ABSTRACT. The propagation of elastic waves in a material can involve a number of complex physical phenomena, resulting in both subtle and dramatic effects on detected signal content. In recent years, the use of advanced methods for characterizing and imaging elastic wave propagation and scattering processes has increased, where for example the use of scanning laser vibrometry and advanced computational models have been used very effectively to identify propagating modes, scattering phenomena, and damage feature interactions. In the present effort, the propagation of Lamb waves within a narrow, constrained geometry composite pi-joint structure are studied using 3D finite element models and scanning laser vibrometry measurements, where the effects of varying sample thickness, complex joint curvatures, and restricted structure geometries are highlighted, and a direct comparison of computational and experimental results are provided for simulated and realistic geometry composite pi-joint samples.

Keywords: Composite Joint, Lamb Waves, Scanning Laser Vibrometry, Finite Element Modeling
PACS: 43.35.Pt; 81.70.-q; 43.35.Bf

INTRODUCTION

In recent years, the use of composite materials in aircraft structures has increased, where for example the newly developed Boeing B787 and Airbus A350-XWB aircraft are expected to contain nearly 50% composite materials [1]. With increased composite material use, the need for structural integrity and damage assessment in these important materials has also increased, where ultrasonic sensing using guided Lamb waves has drawn considerable interest [2-4]. As pointed out by Giurgiutiu [5], the appeal of guided Lamb waves involves its capability for accomplishing measurements over extended regions with a minimal number of sensors. Combined with the availability of inexpensive piezoelectric sensor disks, the efficient generation and use of guided Lamb waves for damage detection, location, and quantification in thin-walled plates and shells is showing continued promise for use many practical applications.

1

The use of guided Lamb waves has been studied extensively, with an increasing emphasis on the detection of damage in composite laminate materials [6-9]. In much of the work done to date, however, guided wave sensing has focused on large, open, plate-like structures typically found in wings and fuselage structures [10]. Although these structures are of concern for aerospace applications, structural joints are historically of critical importance for aircraft structural integrity assessments [11]. An increasing need exists, therefore, for sensing technologies capable of characterizing complex geometry and localized joints in composite structures.

In this paper, the characterization of a restricted geometry composite joint is studied using Lamb waves generated by bonded piezo sensor disks. The sensors were strategically placed on either side of the composite joint, which included a varying thickness, multi-layer composite structure with a vertical riser. Finite element models and scanning laser vibrometry measurements were used to study the generation and propagation of Lamb waves in the material, where both undamaged and damaged specimens are considered. Extensive use of forward models were used to understand Lamb wave interactions with the structure, where scanning laser vibrometry measurements were used as a method for model validation. The remainder of the manuscript includes a brief technical background on Lamb wave sensing in a restricted geometry composite joint, followed by a description of the forward models, experimental studies, results, and conclusions.

LAMB WAVE PROPAGATION IN A RESTRICTED GEOMETRY PI-JOINT

Physics of Wave Propagation Problem

Guided Lamb waves involve the propagation of elastic waves in a bounded medium whose particle motion lies in the plane defined by the plate normal to the direction of wave propagation [12]. In contrast to bulk waves, guided Lamb waves involve two infinite sets of propagating modes, referred to as symmetric S_n and antisymmetric A_n modes. In most instances, the S_n and A_n modes are dispersive in nature, where the velocity of a propagating mode, c_n, depends on the ultrasonic frequency, the elastic constants and density of the material, and the ratio of the plate thickness, d, and propagating mode wavelength, λ, which determine the effective stiffness of the plate [2,3,12]. For a given thickness d and frequency f, the characteristic propagating modes and wave velocities can be established using dispersion curves calculated from the Rayleigh–Lamb relations [2,3,12].
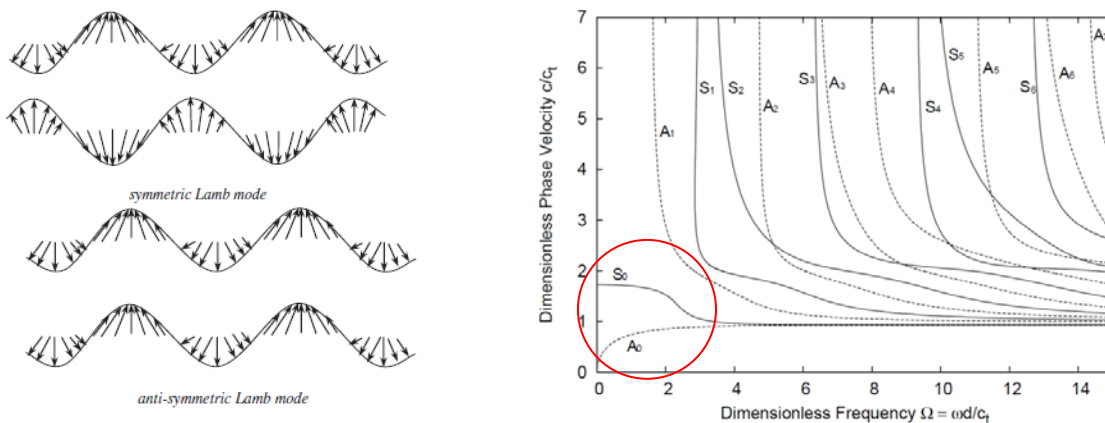

FIGURE 1. Schematic diagram of symmetric and antisymmetric guided Lamb wave modes (left), and example of dispersion curve for propagating modes in a thin-walled, plate structure (right).

It is widely known that the phenomenon of velocity dispersion can lead to significant complexity with respect to experimentally observed Lamb wave signals. As a result, the use of single mode, or 'tuned', excitation methods have been developed, where a single fundamental mode is preferentially excited and other modes are suppressed. As originally described by Giurgiutiu [5], the direct shear-layer coupling between an adhesively bonded piezoelectric sensor disk and a structure can lead to an inherent and preferred coupling of energy into a particular Lamb wave mode by frequency tuning. This represents a key feature for minimizing signal complexity in a practical Lamb wave measurement process when geometric/material complexity exists (Figure 2). The fundamental A_0 mode, for example, can effectively be isolated for generation and detection purposes, where previous research has shown signal content simplification and enhanced interactions of A_0 energy with delaminations in composite laminates [5].
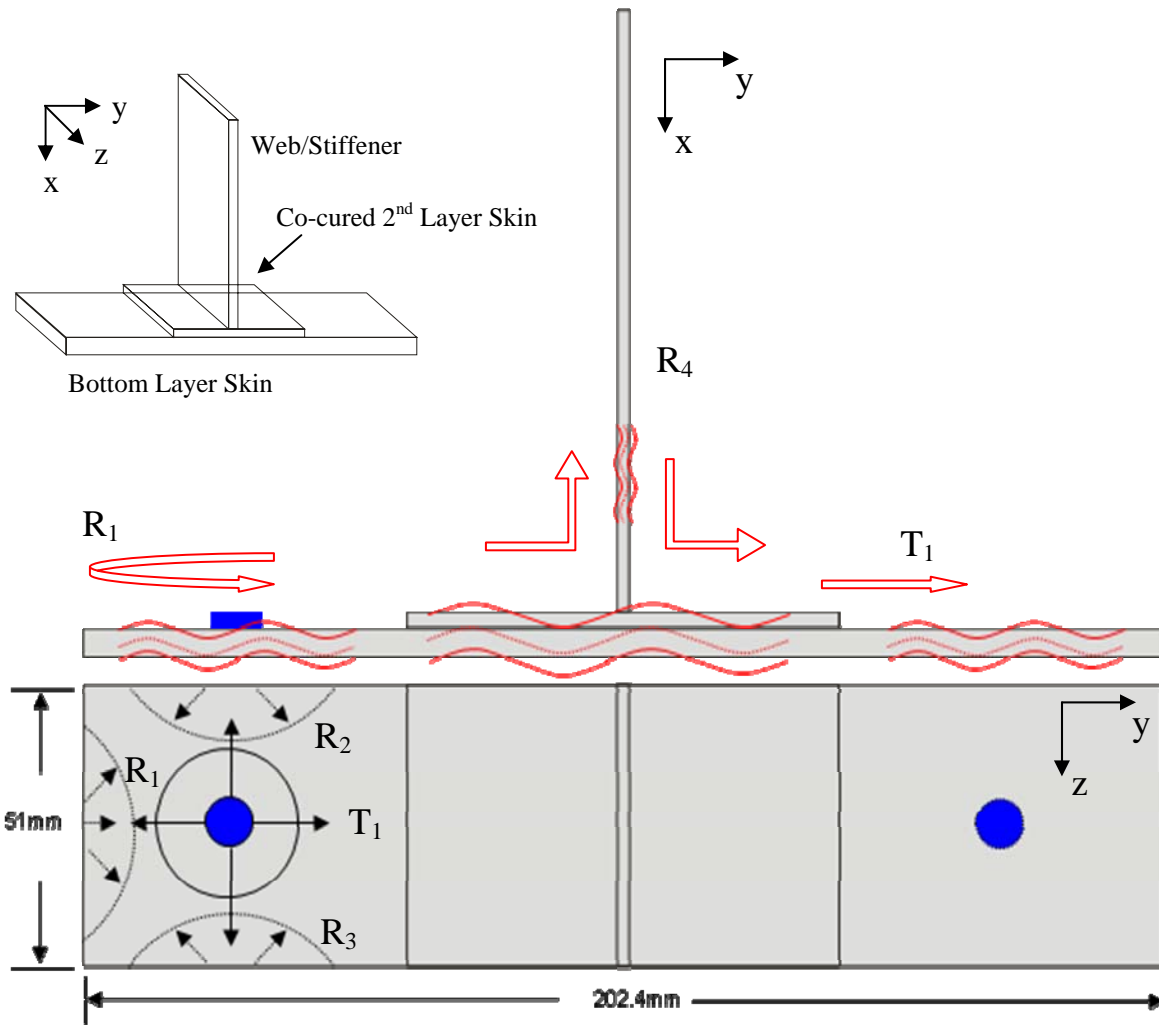

FIGURE 2. Schematic diagram of thin 2-layer, restricted-geometry joint with a vertical web attachment. A schematic representation of the piezo disk sensor placement and propagating guided waves are also depicted where guided Lamb waves propagate in the thickness of the sample in the X-Y plane (top schematic view), and omnidirectional waves propagate away from the sensor in the Y-Z plane (bottom schematic view).

With regard to wave propagation in the restricted geometry sample depicted in Figure 2, several important points can be made. For low-frequency waves of f = 100kHz, the propagating modes are restricted to the two lowest modes A_0 and S_0 depicted in the dispersion curve diagram of Figure 1. In addition, mode selection can be used to

3

preferentially excite A_0 versus S_0 [5,13], where a single A_0 mode exists within the material volume. For the composite material used in the current study (a carbon fiber reinforced polymer, CFRP), wavelengths and phase velocities for the A_0 mode were near 10 mm and 1500 m/s, respectively. Due to the restricted sample geometry, reflective waves are quickly generated at the left end (R_1) and top-bottom sidewalls (R_2 and R_3) of the sample in the axial-transverse plane (Y-Z). These reflected waves propagate and superposition within the 3D volume in a semi-coherent nature, resulting in signal content trailing behind the direct-transmit wave (T_1) with 25-100 microsecond time delays for detection positions along the sample length. The variation and increase of thickness in the co-cured joint region can also cause shifts in the frequency-thickness product (see Figure 1), with corresponding changes in the phase velocity, c_p, and wavelength, λ, of the propagating modes in those regions. Propagation and re-direction of energy into the vertical web region can also occur (Figure 2), with mode conversion and additional dispersive characteristics at the various reflective surfaces (R_4) and thickness variation positions.

Numerical Modeling Approach and Studies

A series of 3D-finite element models were used to study the behavior of the Lamb wave interactions within the composite joint depicted in Figure 3. The model was developed in a commercially available finite element package PZFlex, which is designed and optimized for elastic wave propagation analysis. The model geometry depicted in Figure 3 was chosen to match as closely as possible the cross-sectional profile and 3D characteristics of a composite joint sample used in mechanical testing studies. Figure 3 provides a schematic cross-sectional diagram of the composite joint test article, and digital images of a sample showing bonded piezo sensors and composite layers in cross-section. The sample included a 40-ply, quasi-isotropic lay-up [0/90/45/-45]5S for the graphite fiber/epoxy composite skin (Newport Adhesives and Composites, NCT-350-GT145-TR50S), which was co-cured with a 20-ply vertical riser/web lay-up [0/45/90/-45/-45/45/45/90]S, where ½ of the web plies were split and re-directed 90-degrees into the top surface of the skin during the curing process [14]. The overall length, width, and thickness of the skin region were 202.4 mm, 51 mm, and 4.8 mm, respectively. In the overlap region of the skin, the thickness increases to 6.6 mm due the additional 2 composite plies, while the thickness of the vertical riser/web region was 2.45 mm with an overall height of 140 mm. The thickened region extends out ~42.8 mm on either side of the vertical riser/web region along the length of the sample. As shown in the inset images and schematic diagram in Figure 3, piezoelectric sensors (APC D-6.35mm-0.2mm-850WFB) were bonded on the top and bottom surfaces of the composite skin, with four additional sensors placed symmetrically on either side of the web. The sensors were bonded to the specimen using M-Bond adhesive, and were located along the length and height of the specimen as depicted in Figure 3. The sensors were 6.35 mm round disks of PZT, with a thickness of 200 microns, and were polarized to produce a radial shearing force when actuated.

The 3D finite element model used to approximate the realistic sample geometry included a 200 mm long x 50 mm wide x 140 mm high structure (see upper right inset graphic in Figure 3). A single piezoelectric sensor (PZT:fpz29) was used to generate Lamb waves in the model and was located on the top left surface of the skin as depicted in Figure 3. The sensor had a diameter of 6.35 mm and a thickness of 250 microns. A hard epoxy bonding layer 250 microns thick was used in the model to couple energy into the composite. The model had a grid element spacing of 250 microns, which resulted in 560 x 800 x 100 = 44,800,000 elements. A symmetry plane was located at the midpoint of the sample in the transverse direction (z-plane) extending along the sample geometry length.
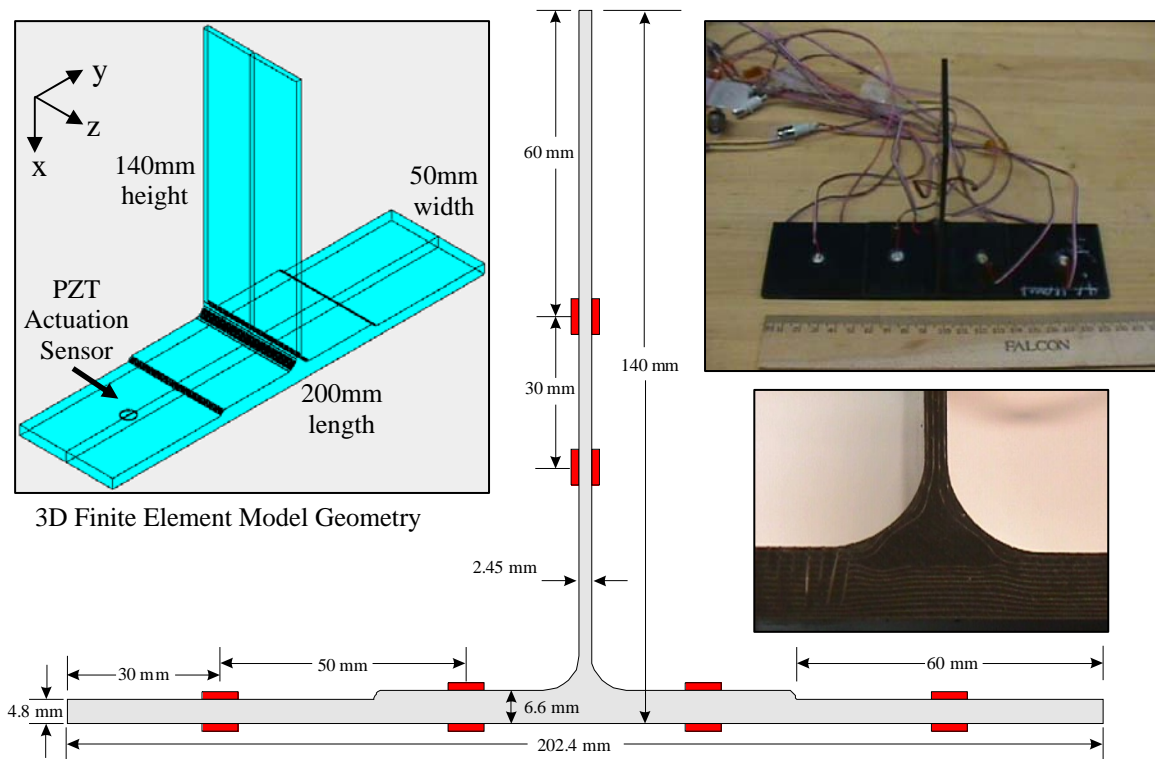
4

FIGURE 3. Schematic of 3D finite element model geometry (upper left), cross-sectional details (center), and digital images of specimen (right).

The material properties of the composite were treated as being isotropic and homogeneous in the current model with a density of 1500 kg/m^3, a longitudinal velocity of 3946 m/s, and a shear velocity of 1941 m/s. Free-boundary conditions were applied to all of the exposed surfaces of the model. The excitation pulse and FFT spectrum for the 100 kHz excitation used in the model are depicted in Figure 4, respectively. Discretization of the domain was set to 60 elements per wavelength, which provided adequate stability and convergence of the model, and an accurate representation of the Lamb wave propagation and scattering features. Model run times were typically 200 usec with a Dt = 0.0397 usec.
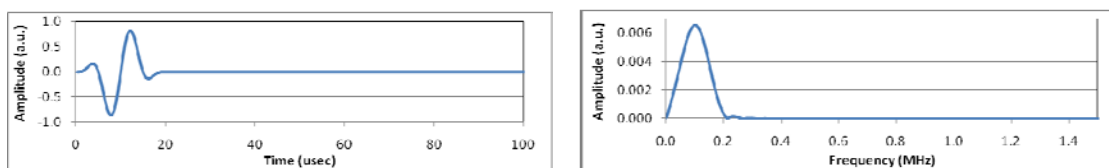

FIGURE 4. Finite element model 100 kHz excitation signal (left), and its frequency spectrum (right).

Figures 5 and 6 depict model results for the composite joint studies. Figure 5 depicts x-displacement component amplitude levels for different time steps between 11.9 usec and 111.1 usec, where circularly symmetric wave can be seen propagating away from the piezoelectric actuator location with reflections from the sides and left end of the sample occuring at 20 usec and 30 usec, respectively. Figure 6 depicts x-displacement amplitude levels occuring on the top and bottom surfaces of the sample, where anti-symmetric motions occur between the two surfaces, consistent with A_0 mode propagation. Figure 6 also depicts a B-scan image (left bottom) and a detected signal (right bottom) for the y,z = (60mm, 25mm) position, where an A_0 phase velocity of 1485 m/s was estimated. Reflected wave features due to the restricted geometry are observed in both cases for R_1, R_2, and R_3.
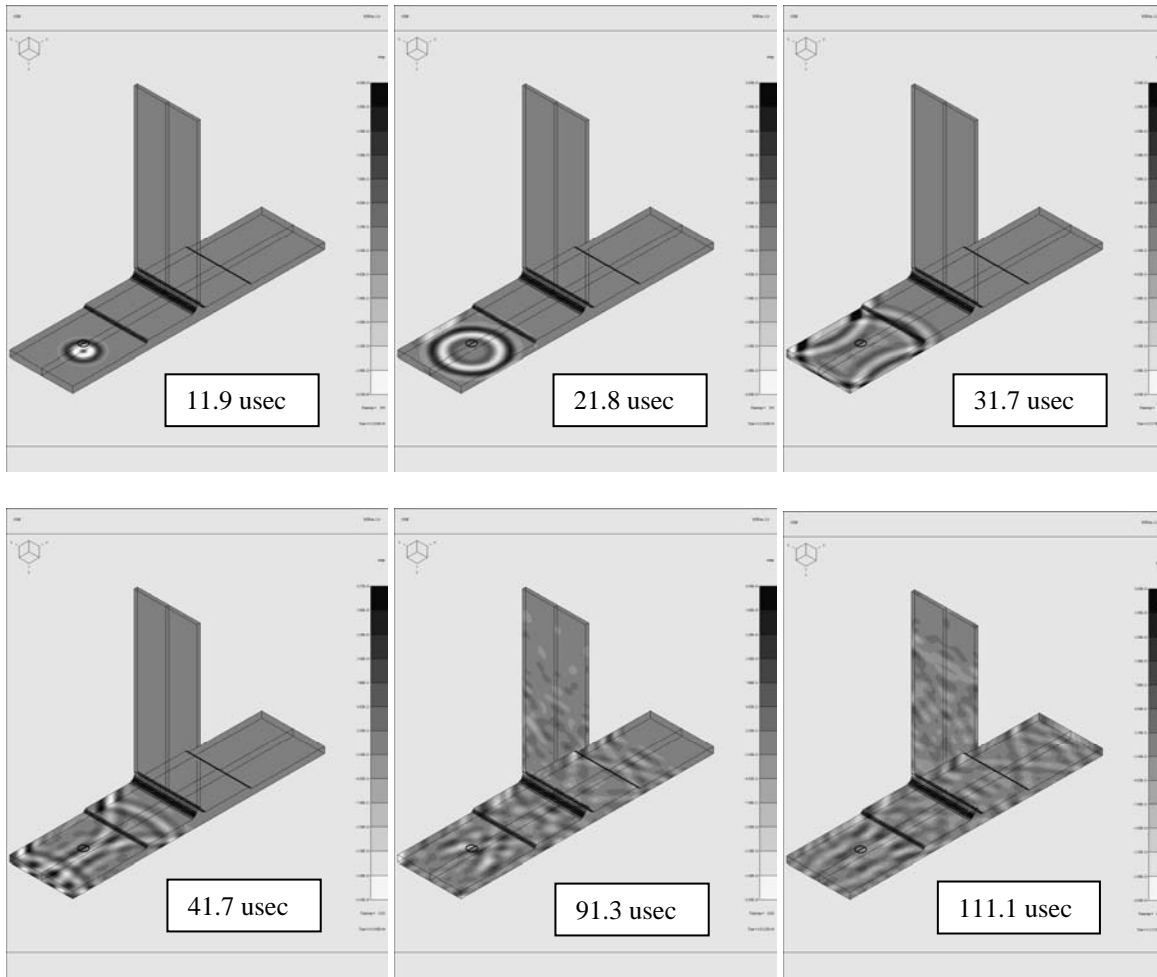
5

FIGURE 5. Model-based x-displacement amplitudes for 3D composite joint at increasing times.
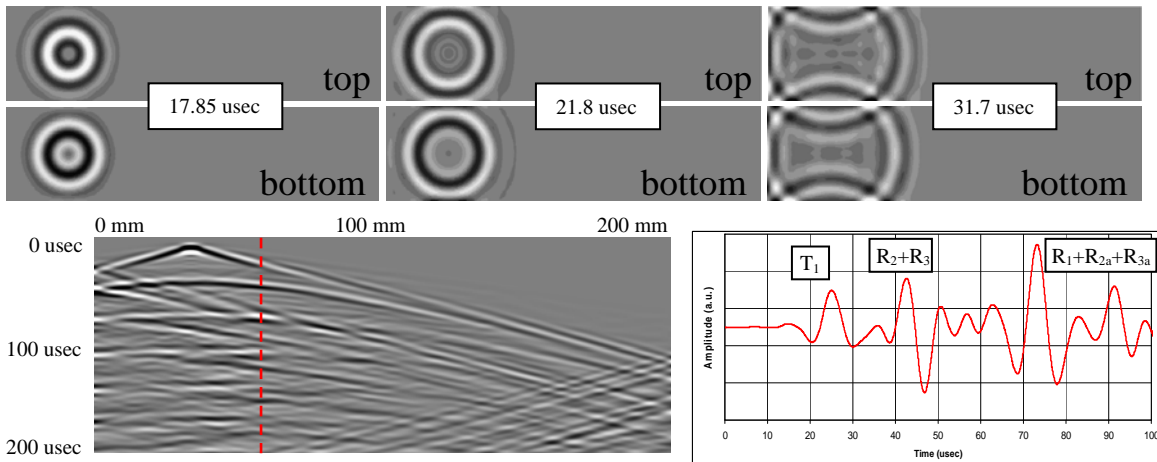

FIGURE 6. X-displacement model results: top/bottom skin surface images (top), B-scan for centerline of bottom surface (bottom left), and detected signal at y,z = (60mm, 25mm) on bottom surface (bottom right).

Model Validation using Scanning Laser Vibrometry

In recent years, the use of advanced methods for characterizing and imaging elastic wave propagation and scattering processes has increased, where for example the use of scanning laser vibrometry (SLV) has been used very effectively to identify propagating

6

modes, scattering phenomena, and damage feature properties [15,16]. A typical scanning laser vibrometry system provides a means for measuring the local velocity or displacement levels on a material surface with spatial resolutions approaching 1 micron. In the present effort, a scanning laser vibrometry system was used as a validation tool for the finite element modeling results presented in the previous section.

Figure 7 provides a comparison of model generated and scanning laser vibrometry measurement results for the bottom surface of the 3D composite joint specimen. A single bonded piezoelectric sensor disk was used to generate Lamb waves in the sample for the SLV measurements at the same location on the top skin used in the model studies (see Figure 3). Three examples of the ultrasonic displacement field are shown in Figure 7 (top sets of images) for the x-displacement on the bottom surface of the composite skin. Good agreement is observed between the propagation speeds and wave characteristics in all three cases. A comparison of B-scans extracted for the x-displacement along the centerline of the bottom surface of the composite skin is presented in Figure 7 (center set of images). Reasonable agreement between the model and experimental measurements is again observed. Estimations of the A_0 phase velocity were made using the B-scan results and were 1485 m/s and 1462 m/s for the model and scanning laser vibrometry signals, respectively. A comparison of x-displacement signals at y,z = (0mm, 25mm) and (100mm, 25mm) are shown in the bottom left and right plots in Figure 7, respectively, where good qualitative agreement is seen in the results.
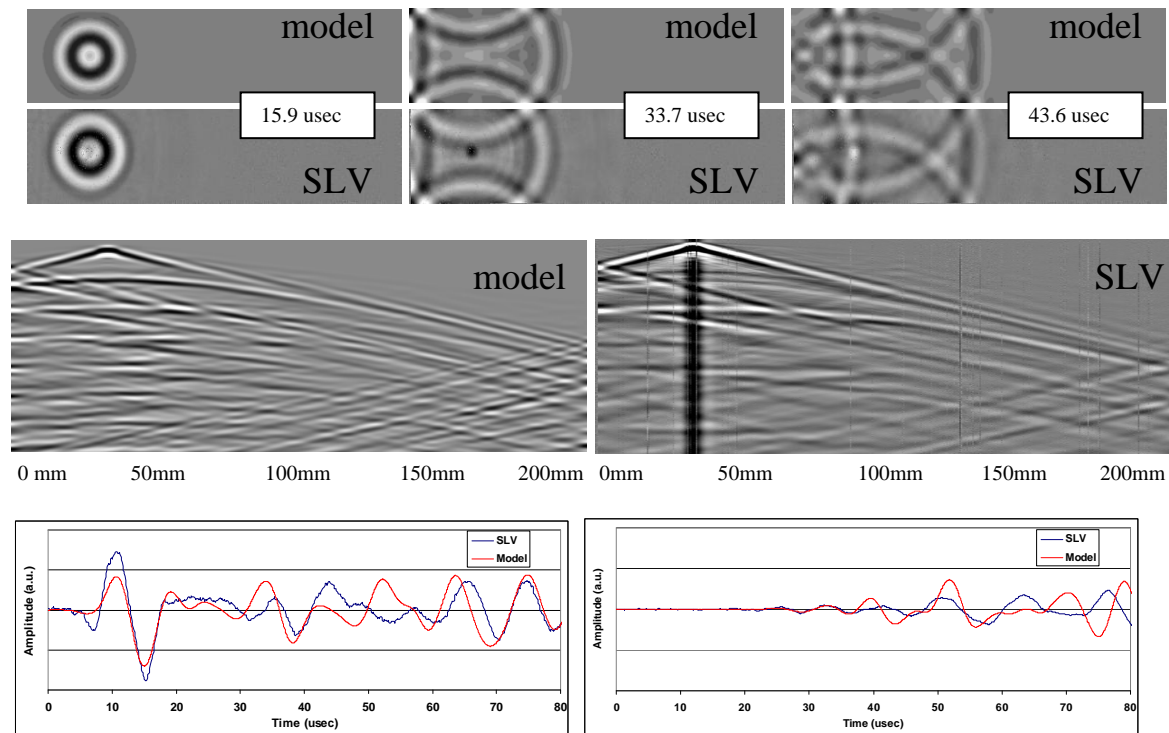

FIGURE 7. Comparison of finite element model and scanning laser vibrometry results; x-displacement images (top), B-scans for centerline of bottom surfaces (center), and signals at 50 mm and 100mm (bottom).

CONCLUSIONS

The present research utilized finite element analysis models to study Lamb wave propagation and scattering in a restricted geometry composite structural joint. Selective mode tuning with a 100 kHz pulse generated the lowest order antisymmetric A_0 mode in the structure, which was verified by comparing model-generated displacement fields on

7

the top and bottom surfaces of the composite skin. Due to the restricted geometry conditions, which included a 50 mm wide by 200 mm long composite structure, significant reflections occurred in the sample, which were semi-coherent in nature and were distinguishable in the modeling results through B-scan and displacement signal analysis. Validation of model predictions was accomplished using scanning laser vibrometry measurements, where excellent agreement was seen for model versus experimental results for displacement field images, B-scan analyses, and displacement signal content.

REFERENCES

1. Croft, J., "Airbus and Boeing Spar for Middleweight Title," Aerospace America, pp. 36-42, July 2005.
2. Adams, D., Health Monitoring of Structural Materials and Components, John Wiley and Sons, New Jersey, 2007.
3. Giurgiutiu, V., Structural Health Monitoring with Piezoelectric Wafer Active Sensors, Elsevier, New York, 2008.
4. Staszewski, W. J., Mahzan, S. and Traynor, R., "Health Monitoring of Aerospace Composite Structures – Active and Passive Approach", Composite Science and Technology, Vol. 69, pp. 1678–1685, 2009.
5. Giurgiutiu V., "Tuned Lamb Wave Excitation and Detection with Piezoelectric Wafer Active Sensors for Structural Health Monitoring", Journal of Intelligent Materials Systems and Structures, Vol. 16, No. 4, pp. 291-305, 2005.
6. Kessler S. S., Spearing S. M. and Soutis C., "Damage detection in composite materials using Lamb wave methods, Smart Materials and Structures, v11, pp. 269-278, 2002.
7. Su Z., Ye L., and Lu Y., "Guided Lamb Waves for Identification of Damage in Composite Structures: A Review", J. of Sound and Vibration, v295, pp. 753-780, 2006.
8. Raghavan, A., and Cesnik, C., "Review of Guided-Wave Structural Health Monitoring," The Shock and Vibration Digest, Vol. 39, No. 2, pp. 91-114, 2007.
9. Wang L. and Yuan F. G., "Group velocity and characteristics wave curves of Lamb Waves in Composites: Modeling and experiments", Composite Science and Technology, Vol. 67, pp. 1370-1384, 2007.
10. Dalton, R., Cawley, P., and Lowe M., "The Potential of Guided Waves for Monitoring Large Areas of Metallic Aircraft Fuselage Structures," J. Nondestructive Evaluation, Vol. 20, No. 1, pp. 29-46, 2001.
11. Russel, J.D., "Composite Affordability Initiative: Transitioning Advanced Aerospace Technologies through Cost and Risk Reduction," AMMTIAC Quarterly, v1, n3, 2007.
12. Viktorov, I., Rayleigh and Lamb Waves: Physical Theory and Applications, Plenum Press, New York, 1967.
13. E. Swenson, H. Kapoor, and S. Soni, "Effects of Z-Pins on Lamb Waves in Composite Plates," SPIE Vol. 7649, 2010.
14. Freel J. K., "Modeling fracture in z-pinned composite co-cured laminates using smeared properties and cohesive element in Dyna-3D", Air Force Institute of Technology, MS Thesis, Sept. 2006.
15. Leong, W., Staszewski1, W., Lee, B., and Scarpa, F., "Structural health monitoring using scanning laser vibrometry: III. Lamb waves for fatigue crack detection", Smart Mater. Struct., Vol. 14, No. 6, 2005.
16. Longo, R., Vanlanduita, S., Vanherzeelea, J., and Guillaumea, P., "A method for crack sizing using Laser Doppler Vibrometer measurements of Surface Acoustic Waves", Ultrasonics, Vol. 50, No. 1, pp. 76-80, 2010.